Journal of Low Temperature Physics, Vol. 131, Nos. 3/4, May 2003 (© 2003)

X-ray absorption spectroscopy of CuO_2 chains

S.-L. Drechsler, Z. Hu, J. Málek*, H. Rosner+, R. Neudert, M. Knupfer, M.S. Golden, J. Fink

Leibniz-Institut f. Festkörper- und Werkstofforschung Dresden, P.O. Box 270116, D-01171 Dresden, Germany, Institute of Physics, ASCR, Czech Republic*
+Department. of Physics, University of California, Davis, CA, 95616, USA

The electronic structure of various edge-shared chain compounds $A_{1-x}CuO_2$ (A=Ca,Sr,Ba) was studied by O-K and Cu-L_3 x-ray absorption spectroscopy and exact diagonalizations techniques. The doping-dependent behaviour in these chains differs from that of conventional 2D Cu-O networks of corner-shared CuO_4 plaquettes due to the much smaller inter-plaquette hybridisation. This results in different final states in the Cu-L_3 spectra and a strong reduction in the dynamic spectral weight transfer from the upper Hubbard band to the low energies in the O-K spectra. The spectra can be used to 'read-off' the Cu valency.
PACS numbers: 78.70.Dm, 71.27+a, 71.10-w.

We present a joint experimental (O-K and Cu-L_3 x-ray absorption spectroscopy (XAS)) and theoretical study of the electronic structure of edge-shared $A_{1-x}CuO_2$ chain compounds (ESCS): $Ca_{0.83}CuO_2$, $Sr_{0.73}CuO_2$ and $Ba_{0.67}CuO_2$, whose *edge-shared* CuO_4 plaquettes form CuO_2 chains doped with $2x$ holes per Cu.[1,2] The ESCS provide a unique opportunity among the cuprates to consider the doping dependence of the dynamical spectral weight transfer (DSWT)[3,4] within an unusually broad accessible doping range and under the specific conditions of nearly 90° Cu-O-Cu bonds. Remarkably, the magnetic susceptibility of $Ca_{0.83}CuO_2$ and $Sr_{0.73}CuO_2$ - despite their high hole-doping - can be described within the dimerized alternating spin-1/2 Heisenberg-chain model[1] with antiferromagnetic order setting in at low temperature. For 2D cuprates, neither Néel nor any other long-range magnetic order has been found for high doping levels beyond 0.13 holes per Cu.

For synthesis and structural analysis of our polycrystalline samples see Refs. 1,2. The XAS studies were performed at BESSY-I using fluorescence-yield (FY) and total electron yield (TEY) modes.[5] The XAS-data were sim-

0022-2291/03/0500-0369/0

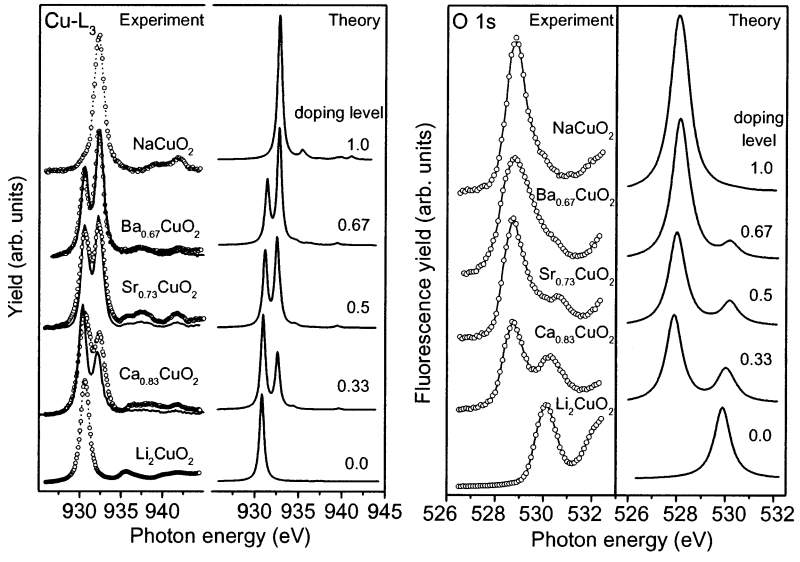

Fig. 1. Left panel: Cu-L_3 XAS spectra of ESCS vs. hole doping. Right panel: simulated spectra using an extended five band *pd* Hubbard model. For the partially doped $A_{1-x}CuO_2$ ESCS (A= Ba,Sr,Ca) we compare fluorescence yield (FY) and total electron yield (TEY).
Fig. 2. The same as in Fig. 1 for the O-K (O 1s) XAS spectra.

ulated with the aid of an extended 5-band *pd* Hubbard-model.[6,7] In our calculations the ground state of the doped chains conserves the translational symmetry of the undoped system. The XAS-spectral densities were calculated by means of the exact diagonalisation of periodic $(CuO_2)_n$ clusters (n=3,4) and the continued fraction technique.[6]

Fig. 1 shows the doping dependence of our XAS spectra. Data from Li_2CuO_2 and $NaCuO_2$ serve as formally di- and trivalent reference systems for the ESCS. Their spectral signatures are white-lines at 930.7 eV and 932.4 eV ascribed to the $2\underline{p}3d^{10}$ configuration ($2\underline{p}$ denotes the core hole) and to $2\underline{p}3d^{10}\underline{L}$ (Ref. 8), respectively. $Ba_{0.67}CuO_2$, $Sr_{0.73}CuO_2$, and $Ca_{0.83}CuO_2$ show nearly coinciding TEY and FY data in contrast to often observed significant differences.[9] Fig. 1 shows that the ESCS with non-integer doping exhibit a Cu-L_3 XAS spectrum which resembles a superposition of the reference spectra. Hence, for non-integer doped ESCS the low and higher energy peaks stem from $2\underline{p}3d^{10}$ and $2\underline{p}3d^{10}\underline{L}$ final states, respectively. The weight of the higher energy peak increases with doping.

It is instructive to compare the Cu-L_3 XAS spectrum of $Ca_{0.83}CuO_2$ with that of the nominally isovalent 2D corner-shared $La_{1.66}Sr_{0.34}CuO_4$[10]: $Cu^{+2.34}$. However, in the latter the higher energy component turns to be a

very weak shoulder.[10] The clear differences between the spectra of nominally isovalent compounds points to the crucial role of the Cu-O network geometry, not only in the Cu-L_3 core level photoemission spectra,[11,12] but also in Cu-L_3 XAS[13]. In the ESCS the Cu-O-Cu interaction pathway is essentially 90°, which strongly suppresses the inter-plaquette hybridisation. Therefore the undoped Li_2CuO_2 is reminiscent to compounds with nearly isolated CuO_4 plaquettes[14]. The XAS of ESCS cuprates resembles some mixed valent $4f$ compounds in which the intensity ratio of features at the (Ln)-L_3 thresholds measures the average valence.[15] For ESCS one observes a clear feature at 932.4 eV in the Cu-L_3 spectra whose weight scales with the nominal Cu valence. In contrast, the systems with strong 180° Cu-O-Cu bonds support significant inter-plaquette hopping which improves the screening of the Cu $2p$ core hole involving the transfer of electron density from ligands away from the ionized core site. As a result, the Cu-L_3 spectra of the nominally isovalent cuprates differ: the ESCS exhibits two clear final state peaks, whereas the corner-shared 2D system shows a mere asymmetry at higher energy.[10]

The consequences of the network geometry-induced effects are not restricted to the Cu-L_3 spectra (see the O-K spectra in Fig. 2). The pronounced peak slightly above the XAS onset at 530.2 eV in the undoped Li_2CuO_2 system is related to transitions into O $2p$ states hybridized with the Cu $3d$ upper Hubbard band (UHB).[16] The pre-edge peak in the O-K XAS spectrum of the trivalent $NaCuO_2$, is assigned to the doped hole states (Zhang-Rice singlet (ZRS)) [10,3,4], is down-shifted by 1.3 eV with respect to the Cu(II) UHB. In hole doped corner-shared 2D systems, two pre-edge peaks on O-K XAS are observed.[10,3] Among them the UHB quickly looses its intensity with increasing doping, whereas the lower energy spectral weight (LESW), the ZRS, increases. The description of LESW was given in Ref. 4. The intermediate-doped ESCS present a different picture (see Fig. 2): (1) as in the case for the Cu-L_3 spectra, the two features remain at the same energies as their counterparts in the nominal Cu(II) and Cu(III) reference systems. (2) the *rate* at which the UHB spectral weight is transferred to the low-energy scale is strongly reduced in the ESCS compared to their corner-sharing 2D cousins. This is much more than an XAS detail, as this spectral weight transfer is an important characteristic of doped cuprates and has been extensively studied in the corner-shared 2D cuprates.[10,17,3,4] There, e.g. in $La_{2-x}Sr_xCuO_4$ [10,3,17] or in the two-leg ladder $La_{1-x}Sr_xCuO_{2.5}$ [18], this effect, i.e. the doping-mediated destruction of the UHB, has been found to be supralinear with x, and has thus been dubbed dynamical spectral weight transfer (DSWT).[4] For example, for $La_{2-x}Sr_xCuO_4$ and x=0.15, the UHB is scarcely visible [10,3] and for the analogous doping level in the two-leg ladder, the UHB-peak has already lost more than 40 % of the spectral weight it had

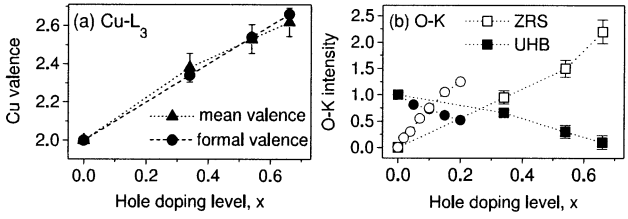

Fig. 3. (a) The mean Cu valence obtained from the Cu-L_3 XAS spectra of $A_{1-x}CuO_2$ and Li_2CuO_2 together with the nominal valence from stoichiometry vs. hole doping, x. (b) the relative intensity of the doping-induced hole peak (ZRS, □), and the UHB (filled □) in the O-K XAS spectra normalized to the intensity of the UHB for undoped Li_2CuO_2 vs. x. UHB (•) and ZRS (○) for $La_{2-x}Sr_xCuO_4$ (from Ref. 3).

for x=0.[18] Here however, for a more as twice as large doping in $Ca_{0.83}CuO_2$, we still find $\sim$ 67% spectral intensity of the UHB compared with the undoped Li_2CuO_2. Even $Ba_{0.67}CuO_2$ still shows a clear UHB feature in the O-K XAS. The suppression of the DSWT is well described by the extended 5-band *pd* Hubbard model [7] (see Fig. 2).[19]

Fig. 3 summarizes our data. The mean Cu valencies from the intensity of the Cu(II)/Cu(III) signals in the Cu-L_3 XAS are compared to the nominal valence from the stoichiometry, yielding an almost perfect agreement. This emphasizes the unique nature of these ESCS which represent the first "mixed valent" cuprate subgroup. XAS allows one to 'read off' the mean Cu valence from the intensity ratio of the Cu-L_3 double-peak. Fig. 3b shows the doping dependence of the spectral weight of the ZRS/UHB in the O-K XAS spectra. Their dependence for $La_{2-x}Sr_xCuO_4$ has been included for comparison. The significant suppression of the DSWT is evident. The general behaviour of the O-K XAS spectra for low-dimensional cuprates, as compared with the Cu-L_3 XAS spectra, is well established.[4] Since the DSWT is independent on cluster size and dimensionality for bandwidth kept fixed, we compare $A_{1-x}CuO_2$ and $La_{2-x}Sr_xCuO_4$ (their bandwidths differ by a factor of ~ 4.[16]). The standard *pd*-model applied to corner-shared 2D CuO_2 clusters reveals for artificially small transfer integrals $t_{pd} \sim 0.5$ eV that the LESW follows the doping linearly.[4] At low doping ($x \leq 0.2$) the LESW develops for O-K spectra of $La_{2-x}Sr_xCuO_4$ nearly twice as fast than for the ESCS $A_{1-x}CuO_2$ (Fig. 3b). Such different slopes have been predicted comparing the cases t_{pd} = 0.5eV and 2eV.[4] Here it is related to the decreasing interplaquette hybridisation ongoing from $La_{2-x}Sr_xCuO_4$ to $A_{1-x}CuO_2$. For $x > 0.2$ no data for 2D cuprates are available to be compared with our ESCS.

To summarize, we studied how hole doping affects the electronic structure of ESCS. (1) The suppression of non-local processes which screen the

core hole in Cu-L_3 XAS results in a mixed valence-like behaviour. The mean Cu valence can be derived from the relative intensity of the final state features. This is an unprecedently clear example of the impact of non-local effects in XAS present in other, corner-shared, cuprates but absent here. (2) The dynamic transfer of spectral weight from the UHB to the low-energy scale is strongly suppressed, resulting in the observation of its feature in the O-K spectra up to a doping of 0.66 holes per Cu. (3) Together with the observation of Néel order in $Sr_{0.73}CuO_2$ and $Ca_{0.83}CuO_2$ (Ref. 1) our data point to individually identifiable $Cu(II)O_4/Cu(III)O_4$ plaquettes in ESCS.

This work was funded by the DFG and the DAAD (H.R.).

REFERENCES

1. G. Meijer et al., *Phys. Rev. B* **58**, 14452, A. Shengelaya et al., *Phys. Rev. Lett.* **80**, 3626 (1998), I.V. Rozhdestvenskaya et al., *Physica C* **311**, 239 (1999).
2. J. Karpinski et al., *Physica C* **274**, 99 (1997).
3. C.T. Chen et al., *Phys. Rev. Lett.* **66**, 104 (1991).
4. H. Eskes et al., *Phys. Rev. Lett.* **67**, 1035 (1993); M.B. Meinders et al., *Phys. Rev. B* **48**, 3916 (1993).
5. For experimental details see: Z. Hu et al., *Europhys. Lett.* **59**, 135 (2002).
6. M. Hybertsen et al., *Phys. Rev. B* **45**, 10032 (1992).
7. The following parameters (in eV) were adopted. Undoped chains: U_d=8.8, U_p=5, t_{pd}=1.4, V_{pd}=1, V_{pp}=0.5, $U_{pp'}$=4 (pp' denotes different O 2p-orbitals at the same site), and U_{cd}=10, and $t_{pp,\parallel} = 0.5t_{pp,\perp}$, where $t_{pp,\perp} = (1/\sqrt{2})((pp\sigma) - (pp\pi))$. To describe the doping effect, alteration of Δ_{pd} and t_{pp} was necessary. We ascribe this to changes of the crystal potential and contraction of the O 2p Wannier functions. In general $t_{pp,\perp} \leq 0.3$ has been adopted. The calculated δ-peaks were broadened with Lorentzians of half-width 0.4 eV.
8. D.D. Sarma et al., *Phys. Rev. B* **37**, 9784 (1988).
9. Our self-absorption correction is meaningful (max. error for the Cu-L_3 intensities $\approx$ 10 %). Larger uncertainty for Li_2CuO_2 and $NaCuO_2$ (energy reference for Cu^{2+} and Cu^{3+} absorption) is irrelevant for our peak ratio analysis: both show a single Cu-L_3 line. Peak energies are unaffected by the correction.
10. C.T. Chen et al., *Phys. Rev. Lett.* **68**, 2534 (1992).
11. M.A. van Veenendaal and G.A. Sawatzky, *Phys. Rev. B* **49**, 3473 (1994).
12. T. Böske et al., *Phys. Rev. B* **56**, 3438 (1997), – *ibid.* **57**, 138 (1998).
13. K. Okada and A. Kotani, *J. Phys. Soc. Jpn.* **68**, 666 (1999).
14. S. Atzkern et al., *Phys. Rev. B* **62**, 7845 (2000).
15. Z. Hu et al., *J. Alloys Comp.* **246**, 186 (1997).
16. R. Neudert et al., *Phys. Rev. B* **60**, 134130 (1999).
17. H. Romberg et al., *Phys. Rev. B* **42**, 8768 (1990).
18. T. Mizokawa et al., *Phys. Rev. B* **55**, R13373 (1997).
19. This knowledge was helpful in our assignment of polarisation-dependent XAS data for $(Sr,Ca,Y,La)_{14}$ with 2-leg ladders and highly doped ESCS (N. Nücker et al., *Phys. Rev. B* **62**, 14384 (2000)).